Electrical Vehicles – Practical Solutions for Power Traction Motor Systems

Mircea Popescu, *Fellow, IEEE,* James Goss, Dave Staton, *Member, IEEE,*

Douglas Hawkins, Yew Chuan Chong and Aldo Boglietti, *Fellow, IEEE*

Abstract—This paper presents various solutions for the power traction motors of electrical vehicles. Equivalent designs to those commercially available on the roads are investigated. Potential simple modifications of the winding configurations and cooling system are studied: (a) flat wire (hairpin) winding vs stranded round wire in induction, synchronous permanent magnet and wound field machine topologies, (b) winding material grades effect – copper vs aluminum, (c) cooling systems – water jacket vs spray, fluid properties and flow rate.

Index Terms— Electrical vehicle, AC motors, permanent magnet motors, induction motors, windings, cooling system

I. INTRODUCTION

THERE is currently wide interest in the research and development of power traction applications driven by electrical machines. On-going efforts are fueled by the need for the new generations of "green" products, such as hybrid and electric vehicles. There are mandatory emission reduction targets for new cars in Europe. The target for 2021 (95% vehicles must achieve targets in 2020 and 100% in 2021) is that all new cars will have maximum 95 grams of CO_2 emission per km fuel consumption of around 4.1 litres/100 km of petrol or 3.6litres /100 km of diesel fuel [1]. Hence, in the drive train only way to achieve targets are drive trains with electric motors [1].

Currently, for electrical vehicles there are solutions using synchronous permanent magnet, synchronous wound field and induction machines. We note that all power traction solutions for electrical vehicles that are currently on the market are of AC type. There are significant research efforts on solutions with reluctance machines: synchronous (also an AC machine) or switched.

Battery Electric Vehicles (BEVs)
A battery electric vehicle uses batteries to power an electric motor to propel the vehicle. The batteries are recharged

M. Popescu, D. A Staton D. Hawkins J. Goss and Y. C. Chong are with Motor Design Ltd., Ellesmere, U.K. (e-mails: mircea.popescu@motor-design.com, dave.staton@motor-design.com, dougie.hawkins@motor-design.com, james.goss@motor-design.com, eddie-chong@motor-design.com).
A. Boglietti is with Politecnico di Torino, Italy, (e-mail: aldo.boglietti@polito.it)

(a) Tesla S [2]

(b) Nissan Leaf [3]

(c) BMW i3 [4]

Figure 1 Battery electrical vehicles examples

from the grid and from regenerative braking.
The advantages of BEVs (Fig. 1) are**:**
° Use of cleaner electric energy produced through advanced technologies or renewable;
° Zero tailpipe emissions;
° Overnight battery recharging;
° Recycled energy from regenerative braking;
° Lower fuel and operational costs;
° Quiet operation
The disadvantages of BEVs are:
° Mileage range;
° Battery technology still to be improved;
° Possible need for public recharging infrastructure

(a) GM Chevrolet Volt [5]

(b) Toyota Prius [6]

Figure 2 Hybrid electrical vehicles examples

Hybrid Electric Vehicles (HEVs)

Hybrid electric vehicles (Fig. 2) are powered by both internal combustion engine and electric motor independently or jointly, doubling the fuel efficiency compared with a conventional vehicle.

A 'parallel' hybrid electric vehicle can use either the electric motor or the internal combustion engine to propel the vehicle. A 'series' hybrid electric vehicle uses the electric motor to provide added power to the internal combustion engine when it needs it most.

The advantages of HEVs are:
° Optimized fuel efficiency and performance;
° Lower fuelling costs;
° Reduced fuel consumption and tailpipe emissions;
° Recovered energy from regenerative braking;
° Use of existing gas station infrastructure

The disadvantages of HEVs are:
° Higher initial cost;
° Complexity of two power trains;
° Component availability—batteries, power trains, power electronics

Hybrid electric vehicles can be classified based on the battery voltage and capacity:
° Micro Hybrid (low voltage 12V): Shuts down engine at idle to save fuel;
° Mild Hybrid (low to medium voltage 12 to 120V): Includes stop-start, regeneration braking, and acceleration assist
° Full Hybrid (high voltage 300V+): All mild HEV features + EV-mode
° Plug-in Hybrid (high voltage 300V+): Recharge battery through electrical outlet

This paper is investigating and comparing various solutions for traction motors in EVs and proposes simple modifications that can improve the motor performance. For relevance, initial designs are based on equivalent existing commercial solutions [2-7]. A comprehensive comparison between existing solutions on the market along with a detailed reference list is given in [8]. Three categories of traction motors are considered, depending on the power level and vehicle type: battery electrical vehicle, plug-in hybrid vehicles, mild hybrid vehicles. The performance improvement or cost reduction can be achieved via various techniques as: flat wire technology winding, oil spray cooling, aluminium winding.

II. BATTERY ELECTRICAL VEHICLES SOLUTIONS

Most of the commercial solutions for the power traction system in BEVs use synchronous permanent magnet motors with embedded rare-earth magnets and distributed stranded wire windings [3,4]. One significant exception is Tesla S that employs an induction motor with copper rotor cage, but also with distributed stranded wire winding. Based on the specifications from Table I. it is possible to investigate the peak and continuous performance of the synchronous PM vs magnet free motor solutions, i.e. induction and synchronous wound field motors. For all design variants, we will consider as alternative the flat wire (hairpin) winding similarly to the solution implemented in Chevrolet Volt [5].

Due to the manufacturing process and the existing tools dedicated to the mass production, it not always recommended or commercially viable to have a completely new design, even if this may be optimized and lead to increased efficiency and/or material costs.

This paper proposes simple modifications of existing solutions, with minimal impact on the production line, that would achieve increased performance. Such easy to implement solutions are related to: (i) Flat wire (hairpin) winding type have not been investigated in magnet-free traction motors: induction or synchronous wound field; (ii) Aluminum as an alternative material for the stator winding; (iii) Efficiency cooling systems with combined water jackets, shaft groove and oil spray elements.

The control strategy and the theory behind the models in this paper are fully described in [9], [10], [12], [17].

TABLE I – BEV POWER TRAIN SPECIFICATIONS

Parameter	Unit	Value
Peak torque	Nm	430
Peak power	kW	270
DC bus voltage	V	366
Maximum speed	rpm	15000
Maximum stator current	Arms	900
Maximum rotor DC current[1]	A	30
Axial active length	mm	150
Motor outer diameter	mm	280
Stator cooling system	N/A	Water jacket (EGW 50/50)
Rotor cooling system[2]	N/A	Shaft grove jacket (EGW50/50)

1) Wound field motor
2) Induction and wound field motor

A. Induction Motor Solution

The main design parameters of the induction motor solution are based on an equivalent to Tesla S 60 traction motor design [2] (see Table II). Fig. 3 shows the radial and axial view of the the induction motor solution. The winding pattern consists of a concentric set of 3 coils per pole and per phase, with a coil pitch of 10-12-14 and turns per coil of 1-2-2. There are two parallel paths in the 3-phase winding system, so that it is possible to supply the motor, if required, from one inverter source (3-phase system) or from two inverter sources (6-phase system). Two winding types are considered: (a) flat wire – hairpin – with 3 rectangular conductors (2.45mm X 3.85mm) in hand forming one turn/coil and (b) stranded round conductors with a wire size AWG # 19 and 25 parallel strands in hand.

The stator lamination is modified accordingly to accommodate the flat wire – parallel slot, and round wire – parallel tooth (Fig. 4). Notice that the wire size and the number of strands in hand correspond to a slot fill factor (copper area/ slot area) equal to 0.35. This is imposed by the automatic procedure of the coils in the stator slots. For a better illustration, in Fig. 4b is shown the model for slots with only one coil inserted. There are 12 slots out of 60 where two coils are inserted and phase separators are required.

The advantage of flat wire winding associated with a parallel slot configuration is a much higher copper slot fill factor [15]. Potential high frequency AC losses in the flat wire conductors can be reduced via twisting/transposition methods [15, 16]. The twisting for flat wires consists in different connections at the end-coil region, so that for example a coil segment placed in a slot opening region is connected to a coil segment placed in a slot end region. For simplicity, this study considers straight conductors, so that AC losses are limited just by the conductors dimensions. There are two main choices when designing an alternative solution with flat wire and parallel slot topology compared to a stranded wire and parallel tooth topology:

(a) Slot area is constant – this helps with considerable reduction of DC copper losses, but has a drawback in the increased copper material weight that is used

(b) Copper area is constant – this helps in reducing the saturation level as the tooth width will increase in flat wire topology, i.e. same copper can fit in a lower slot area due to the higher slot fill factor, but has a disatvantage in increased AC copper losses, while the DC losses are practically constant.

In chosing the slot dimensions, the *overall total area of the slots is kept approximately constant, so that the volume and weight of the stator steel is similar in both designs* (Fig. 4).

The rotor bars are closed and the rotor cage is built using pure copper alloy. For consistency, it is assumed that the rotor cage is die-cast, so that the bars and the end-ring have the same properties, i.e. an electrical resistivity of 1.724 $\mu\Omega$-cm at 20 ^{0}C.

The cooling system comprises two elements: a spiral stator water jacket and a spiral shaft groove. Both elements are using forced convection with water ethylene glycol mixture (50%-50%) as heat extraction fluid and an inlet temperature of 50 ^{0}C. As per the reference [13,14], an induction motor for traction application is proposed to have two cooling systems: one for the stator assembly, one for the rotor assembly. An iterative calculation is performed to identify suitable fluid flow rates for both cooling system and it was considered that a fluid flow rate of 10 liters/min for the stator water jacket and 2 liters/min for the shaft groove respectively would be optimal. In addition, the stator end-winding region is potted with an epoxy type material.

As comparison criteria, the peak and continuous performance are investigated in Figs. 5 – 7. The induction motor is controlled using maximum torque/amp control strategy (MTPA) algorithm with a PWM modulation index of 0.866. The choice for the modulation index corresponds to standard linear range sine/triangle PWM signal and represents the ratio between the peak line-line voltage at the motor terminals and DC bus voltage, neglecting the voltage drop in the inverter switching elements.

The peak performance is modelled considering that the entire motor elements are at a constant temperature of 100^{0}C and peak current 900Arms. Such assumption is practical, as is can be verified on the test bench. Consqently, a similar performance for both types of winding: peak torque of 430Nm achieved up to base speed of 6500rpm. The peak power is 292.6kW @ 6500rpm and 250kW @ 15000rpm (Figs. 5 and 6). However, the efficiency loci shows a slight improvement in the hairpin winding design as the reduction in DC stator copper losses – from maximum 10500W in stranded winding design to maximum 6000W in hairpin winding design - exceeds the increase in high frequency AC stator copper losses – from maximum 2000W in stranded winding design to 5000W in hairpin winding design.

For continuous performance, a coupled model electromagnetic-thermal was used, so that the maximum stator winding temperature does not exceed 180 ^{0}C, which represents industrial insulation class F, while the rotor bearings temperature is limited at 150 ^{0}C. Such limit value for the rotor bearings temperature is usually related to the lubrication and maximum acceptable temperature for the motor grease, that is polyurea based.

TABLE II – BEV INDUCTION MOTOR DETAILS

Parameter	Unit	Value
Stator OD	mm	254
Stator ID	mm	157
Airgap	mm	0.5
Stator Slots	/	60
Poles	/	4
Rotor Bars	/	74
Electric steel	/	M250-35A
Rotor cage	/	Copper

(a) Radial view   (b) Axial view
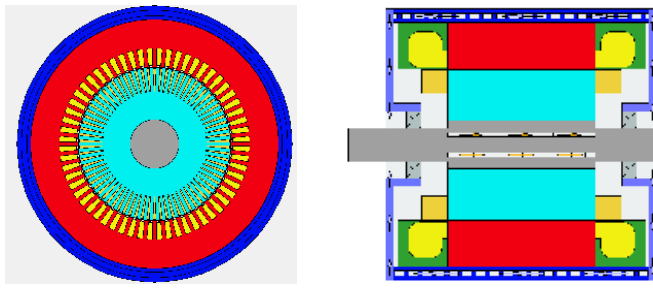
Figure 3 Induction motor design for BEV

(a) flat conductors   (b) stranded conductors
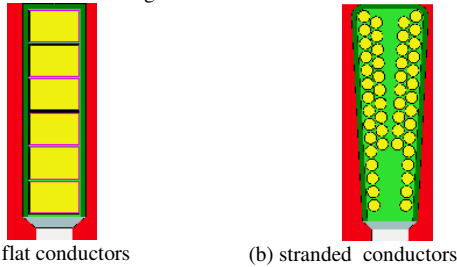
Figure 4 Conductors distribution in the slot of induction motor

(a) IM 1 - hairpin winding

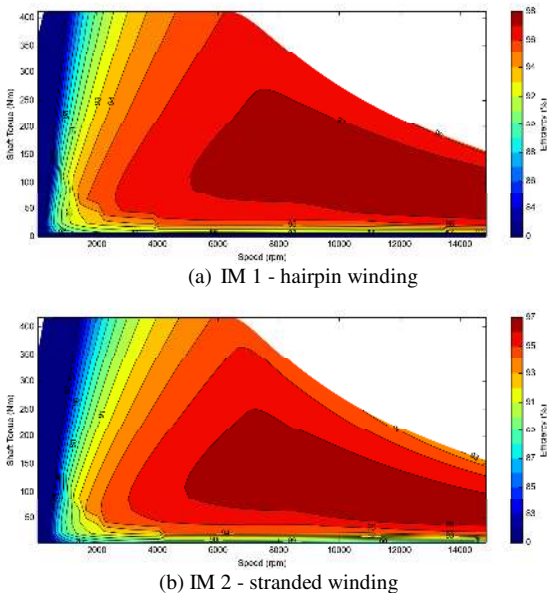(b) IM 2 - stranded winding

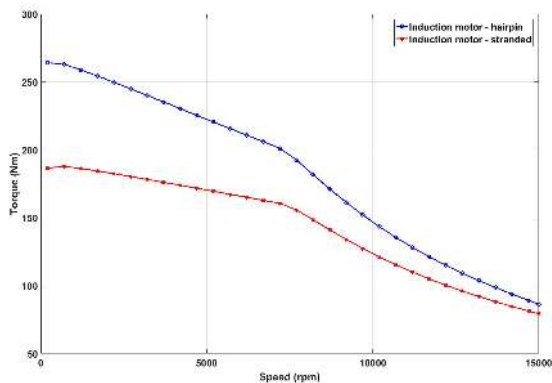Figure 5 Peak torque performance for an induction motor BEV

Figure 6 Continuous torque performance for an induction motor BEV

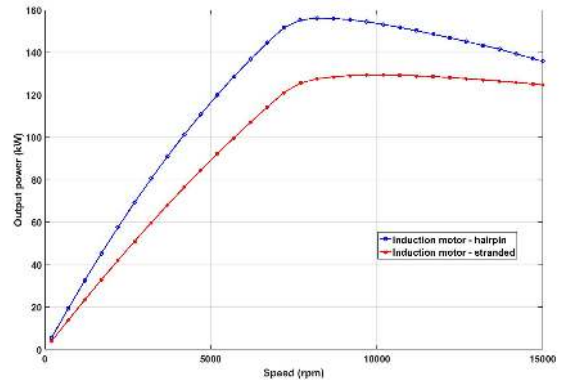Figure 7 Continuous power performance for an induction motor BEV

The continuous performance presented in Figs. 6 and 7, shows the benefits of the flat wire - hairpin winding over the standard round wire winding. When hairpin winding configuration is used and the *same slot area maintained*, the maximum starting continuous torque increases by 44% from 180Nm to 260Nm, while the maximum continuous power sees an increase of 17% from 135kW to 158kW.

For all operation speed range, the limiting thermal factor is the stator winding maximum temperature, i.e. imposed to be 180^0C, related to the corresponding insulation class H.

Within the speed range 0 – 8000rpm, when output power is increasing, the DC copper stator winding loss is the most significant loss component. At higher speed, above 8000rpm, the AC copper stator winding loss increases to a level that leads to a more rapid decrease of the torque for hairpin winding design.

B. Synchronous Interior Permanent Magnet (IPM) Motor Solution

The main design parameters of the synchronous permanent motor solution, are based on a scaled-up equivalent topology to Nissan Leaf traction motor [3, 8] design (see Table III). Fig. 8 shows the radial and axial view of the the synchronous IPM motor solution. The winding pattern consists of a distributed lap set of 1 coil per pole and per phase, with a coil pitch of 5 and turns per coil of 6, see Fig. 9. There are four parallel paths in the 3-phase winding system, so that it is possible to supply the motor if required from one inverter source (3-phase system) or from two inverter sources (6-phase system) or four inverter sources (12-phase system).

Two winding types are considered: (a) flat wire – hairpin – with one rectangular conductor (3.00mm X 4.00mm) in hand forming one turn/coil and (b) stranded round conductors with a wire size 0.71mm and 30 parallel strands in hand. The stator lamination is modified accordingly to accommodate the flat wire – parallel slot and round wire – parallel tooth. In chosing the slot dimensions, *the same the copper area is maintained, so that the volume and weight of the copper winding is similar in both designs*.

The cooling system comprises one element: a spiral stator water jacket using forced convection with water ethylene glycol mixture (50%-50%) as heat extraction fluid and an inlet temperature of 65 ^{0}C. It is assumed a fluid flow rate of 6.5 liters/min. As comparison criteria, the peak and continuous performance are investigated in Figs. 10 – 12. The IPM motor is controlled using the same parameters as for the induction motor. The choice for the modulation index corresponds to standard linear range sine/triangle PWM signal and represents the ratio between the peak line-line voltage at the motor terminals and DC bus voltage, neglecting the voltage drop in the inverter switching elements.

For continuous performance, a coupled model electromagnetic-thermal was used, so that the maximum stator winding temperature does not exceed 180 ^{0}C. The magnets temperature is limited at 140 ^{0}C, corresponding to an operation range recommended by the manufacturers, so that the irreversible demagnetization of the magnet blocks is avoided.

The peak performance at 100^{0}C and peak current 900Arms, is similar for both types of winding: peak torque of 430Nm is achieved up to base speed of 5800rpm. The peak power is 279kW @ 6500rpm and 260kW @ 15000rpm.
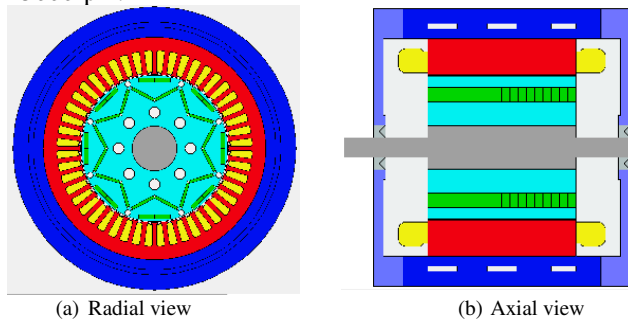

(a) Radial view

(b) Axial view

Figure 8 Synchronous IPM for BEV

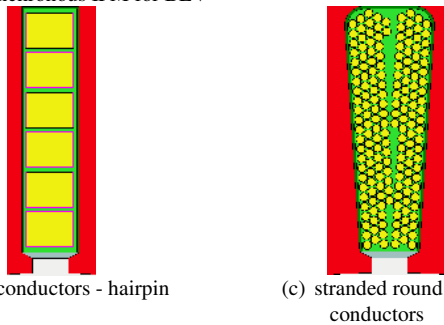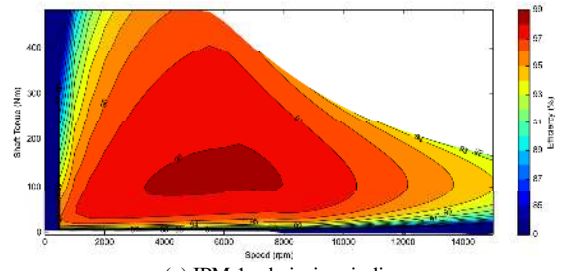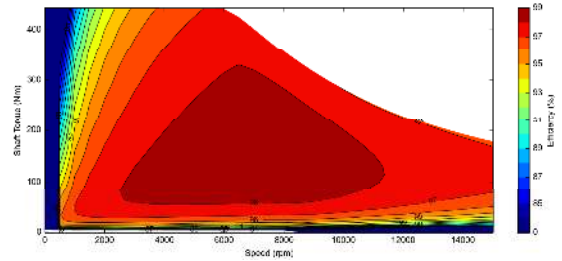(a) flat conductors - hairpin

(c) stranded round conductors

Figure 9 Conductors distribution in the slot of synchronous IPM motor for single layer pattern

TABLE III – BEV SYNCHRONOUS PM MOTOR DETAILS

Parameter	Unit	Value
Stator OD	mm	220
Stator ID	mm	146.67
Airgap	mm	1.0
Slots	/	48
Poles	/	8
Electric steel	/	30 DH
Magnet	/	N35UH

(a) IPM 1 – hairpin winding

(b) IPM 2 – stranded winding

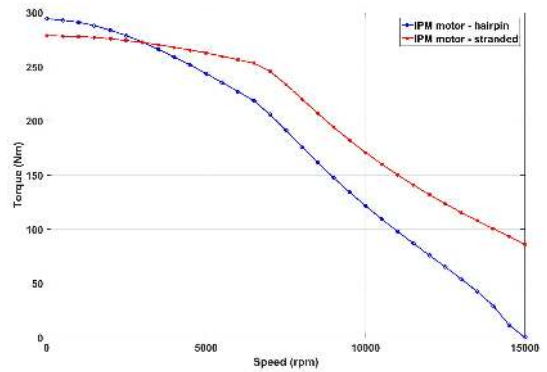Figure 10 Peak torque performance for a synchronous IPM motor BEV

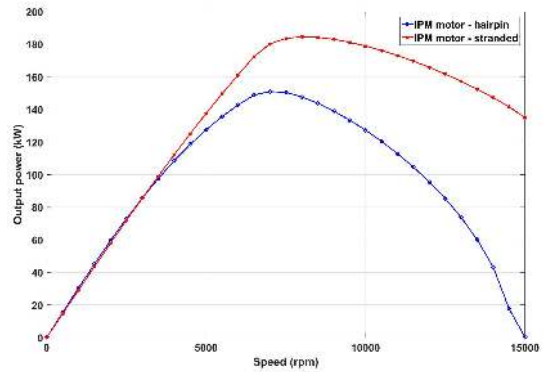Figure 11 Continuous torque performance for a synchronous IPM motor BEV

Figure 12 Continuous power performance for a synchronous IPM motor BEV

However, the efficiency loci shows a lower performance in the hairpin winding design as the DC stator copper losses are practically the same, while the increase in high frequency AC stator copper losses – from maximum 1920W in stranded winding design to 10000W in hairpin winding design.

The continuous performance presented in Figs. 11 and 12, shows that if the same volume of copper is used, there

are performance benefits if using a flat wire, hairpin winding over the standard round wire winding only at low speed region, i.e. starting torque increases by 7.4% from 270Nm to 290Nm. However, when hairpin winding configuration is used and keeping *the same copper cross-section area* with reference to an equivalent stranded wire design, the maximum continuous power sees a decrease of 21% from 182kW to 150kW.

The rapid decrease of torque and power at high speed range for the hairpin winding is due to the higher AC losses in the stator winding.

C. Synchronous Wound Field Salient Rotor Motor Solution

The synchronous wound field salient rotor motor solution is using a similar stator to synchronous IPM motor traction motor design. This includes the same stator lamination radial and axial dimensions, the same winding pattern and wire size. The rotor is designed with same outer diameter as the IPM motor solution, i.e. a similar airgap width is considered. However, the rotor magnetic field is generated by 8 salient magnetic iron poles that carry DC field excitation coils. (see Table IV). Fig. 13 shows the radial and axial view of the the synchronous wound field motor solution. For convenience, the winding data is given again as: distributed lap set of 1 coil per pole and per phase, with a coil pitch of 5 and turns per coil of 6; there are four parallel paths in the 3-phase winding system, so that it is possible to supply the motor if required from one inverter source (3-phase system) or from two inverter sources (6-phase system) or four inverter sources (12-phase system).

The rotor excitation winding has 100 turns/coil with a coil copper area of 79mm^2.

Two winding types are considered: (a) flat wire – hairpin – with one rectangular conductor (3.00mm X 4.00mm) in hand forming one turn/coil and (b) stranded round conductors with a wire size 0.71mm and 30 parallel strands in hand. The stator lamination is modified accordingly to accommodate the flat wire – parallel slot and round wire – parallel tooth. In chosing the slot dimensions, the overall total area of the copper in the slot is kept approximately constant, so that the volume and weight of the copper winding is similar in both designs.

The cooling system comprises two elements:
(a) spiral stator water jacket using forced convection with water ethylene glycol mixture (50%-50%) as heat extraction fluid and an inlet temperature of 65 ^{0}C. It is assumed a fluid flow rate of 6.5 liters/min.
(b) shaft spiral groove jacket using forced convection and sharing the same fluid with the water jacket and the same flow rate and inlet temperature as the stator jacket.

As comparison criteria, the peak and continuous performance are investigated in Figs. 14–16. The synchronous motor is controlled using maximum efficiency algorithm with PWM modulation index of 0.866. The choice for the modulation index corresponds to standard linear range sine/triangle PWM signal and represents the ratio between the peak line-line voltage at the motor terminals and DC bus voltage, neglecting the voltage drop in the inverter switching elements.

For continuous performance, a coupled model electromagnetic-thermal was used, so that the maximum stator and rotor winding temperatures does not exceed 180 ^{0}C.

The peak performance at 100^{0}C and maximum stator current 900Arms and 30A dc rotor field excitation, is similar for both types of winding: peak torque of 430Nm is achieved up to base speed of 5500rpm.

TABLE IV – BEV SYNCHRONOUS WOUND FIELD MOTOR DETAILS

Parameter	Unit	Value
Stator OD	mm	220
Stator ID	mm	146.67
Airgap	mm	1.0
Slots	/	48
Poles	/	8
Electric steel	/	30 DH

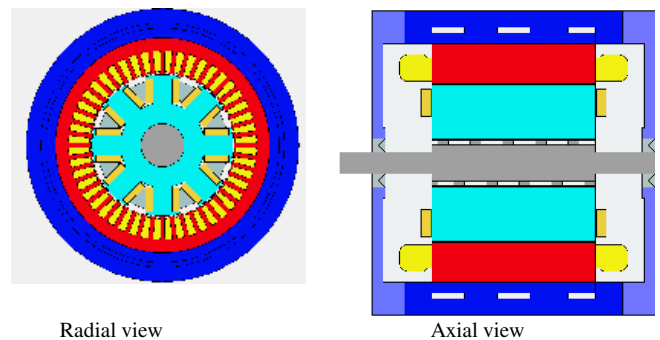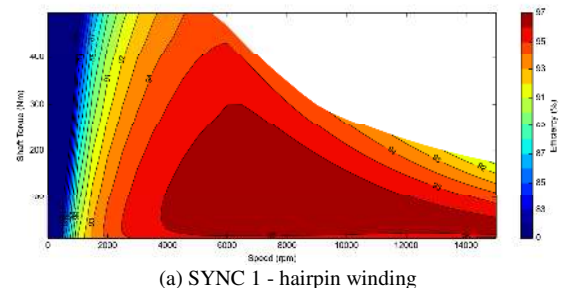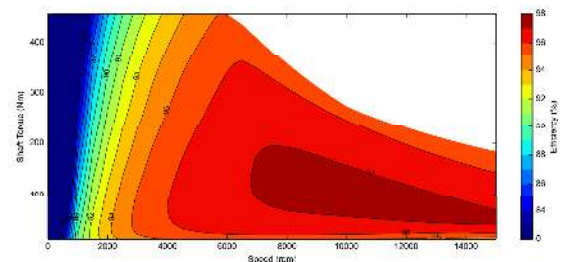Radial view   Axial view
Figure 13 Synchronous wound field motor for BEV

(a) SYNC 1 - hairpin winding

(b) SYNC 2 - stranded winding
Figure 14 Peak torque performance for a synchronous wound field motor BEV

The peak power is 279kW @ 6500rpm and 260kW @ 15000rpm. The continuous performance presented in Figs. 13 and 14, shows that if the same volume of copper is used, the benefits in using a flat wire, hairpin winding over the standard round wire winding are mainly at lower speed,

when a higher torque can be achieved. When hairpin winding configuration is used and keeping the same copper cross-section area, the maximum continuous power decreases by 11% from 139kW to 125kW. The available continuous starting torque increases by 15% from 160Nm to 185Nm.

In summary, the main observations for the BEV solutions are:

(i) A similar peak performance can be achieved with synchronous IPM, wound field or induction motors using the same supply rating (voltage and current);

(ii) The induction motor solution can be 50% heavier than the IPM motor and wound field motor (see Table V);

(iii) The induction motor can deliver higher continuous power at higher speed values, if the fundamental frequency is lower, i.e. lower number of magnetic poles than equivalent PM motor;

(iv) The flat wire winding can lead to significant improvement in performance in induction motors if the same total slot area is used. This is due to the reduced stator DC Joule losses and a better heat extraction with high slot fill factor. Note that the AC Joule losses have a lower impact in the lower number of poles design, if the current time harmonics are neglected. Also, there is an increase in the stator copper weight of approximately 4 kg from 5.52kg – stranded round wire to 9.59kg – flat wire.

(v) The flat wire winding has no advantage in a synchronous wound field motor solution over the design with stranded round wire solution; this is mainly due to the AC Joule losses component.
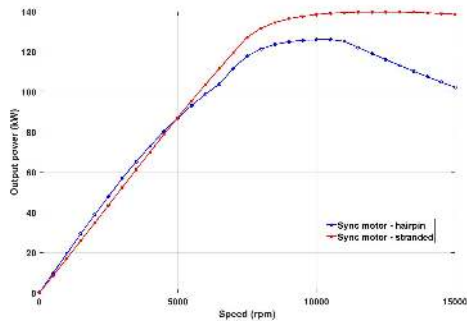
Parameter	IM 1	IM 2	IPM 1	IPM 2	SYNC 1	SYNC 2
Winding wire	Flat	Round	Flat	Round	Flat	Round
Active length (mm)	150	150	150	150	150	150
Stator OD (mm)	254	254	220	220	220	220
Stator copper (kg)	9.59	5.52	7.31	7.31	7.31	7.31
Stator steel (kg)	29.0	28.77	17.9	16.0	17.9	16.0
Rotor steel (kg)	15.5	15.5	12.9	12.9	10.7	10.7
Magnets (kg)	N/A	N/A	2.5	2.5	N/A	N/A
Rotor copper (kg)	9.4	9.4	N/A	N/A	2.6	2.6
Total active weight (kg)	63.7	59.3	42.3	41.4	39.8	38.8

(vi) Induction motor solution is suitable for a flat wire winding if using more copper and less stator iron; in synchronous IPM and wound field motors a flat wire with same copper weight and volume was proved to have benefit only at low to medium speed range.

(vii) Both magnet free solutions, induction and synchronous wound field require a rotor cooling system to match IPM motor performance

III. PLUG-IN HYBRID ELECTRICAL VEHICLES SOLUTIONS

Based on the results from Section II, one possible design for the PHEV specification is a synchronous IPM motor and is based on the equivalent GM Chevrolet Volt [5]. A typical set of specifications is given in Table VI. We can investigate the peak and continuous performance of the synchronous IPM when three cooling system approaches are considered: (a) Stator water spiral jacket; (b) Oil spray cooling; (c) Stator water spiral jacket and oil spray cooling.

The main design parameters of the synchronous IPM motor PHEV solution, are listed in Table VII. Fig. 17 shows the radial and axial view of the the synchronous IPM motor solution.

The winding pattern (Fig. 18) consists of a distributed lap set of 1 coils per pole and per phase, with a coil pitch of 5 and turns per coil of 4. There is one parallel path in the 3-phase winding system. The winding type is considered to be flat wire – hairpin – with one rectangular conductor (4.5mm X 5.00mm) in hand forming one turn/coil.

The cooling system comprises two elements: (a) spiral stator water jacket that is using forced convection with water ethylene glycol mixture (50%-50%) as heat extraction fluid and an inlet temperature of 65 ^{0}C. It is assumed a fluid flow rate of 6 liters/min. (b) oil spray cooling system based
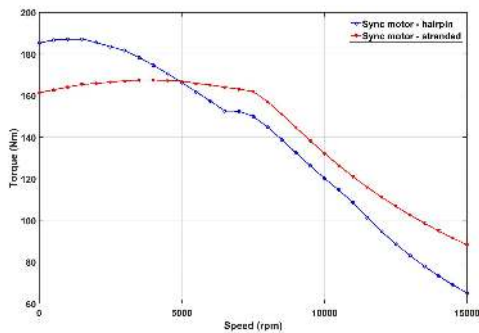

Figure 15 Continuous torque performance for a synchronous wound field motor BEV

Figure 16 Continuous output power performance for a synchronous wound field motor BEV

on that one used by Honda Accord [6] with tubes having 12 nozzles on each side of the motor.

TABLE VI – PHEV POWER TRAIN SPECIFICATIONS

Parameter	Unit	Value
Peak torque	Nm	398
Peak power	kW	110
DC bus voltage	V	366
Maximum speed	rpm	8000
Maximum current	Arms	420
Axial active length	mm	~42.5
Cooling system	N/A	Water jacket (EGW)/Oil spray

TABLE VII – PHEV SYNCHRONOUS IPM MOTOR DETAILS

Parameter	Unit	Value
Stator OD	mm	340
Stator ID	mm	260
Airgap	mm	1.0
Slots	/	72
Poles	/	12
Electric steel	/	M270-35A
Magnet	/	N35UH

(a) Radial view   (b) Axial view
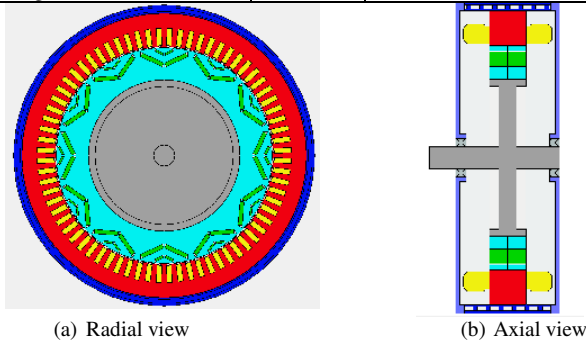
Figure 17 Synchronous IPM for PHEV
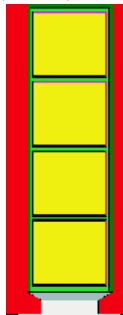
Figure 18 Conductors distribution in the slot of synchronous IPM motor, single layer winding pattern

The oil drips on the end-winding of the motor with a flow rate of 2 liters/min and an inlet temperature of 90 ^{0}C.

As comparison criteria, the peak and continuous performance are investigated in Figs. 19–20. The IPM motor is controlled using MTPA algorithm with PWM modulation index of 0.95. The choice for the modulation index corresponds to a linear range sine/triangle PWM signal with 3rd harmonic injection and represents the ratio between the peak line-line voltage at the motor terminals and DC bus voltage, considering also 5% voltage drop in the inverter switching elements.

For continuous performance, a coupled model electromagnetic-thermal was used, so that the maximum stator winding temperature does not exceed 180 ^{0}C, while the magnets temperature is limited at 140 ^{0}C.

The peak performance with all the motor elements at 100^{0}C and maximum current 420Arms, is similar for all cooling systems: peak torque of 398Nm achieved up to base speed of 3000rpm. The peak power is 125kW @ 3000rpm and 105kW @ 8000rpm (Fig. 19).

The continuous performance presented in Fig. 20, shows the great advantage of the oil spray cooling over a stator spiral water jacket.
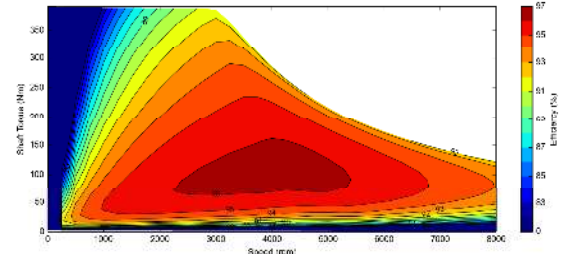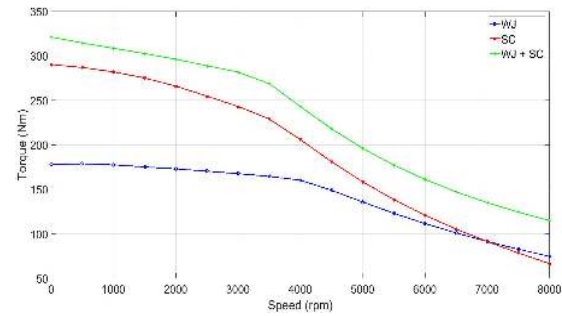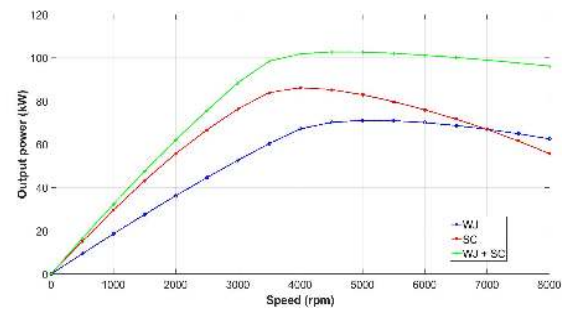

(a) Peak torque
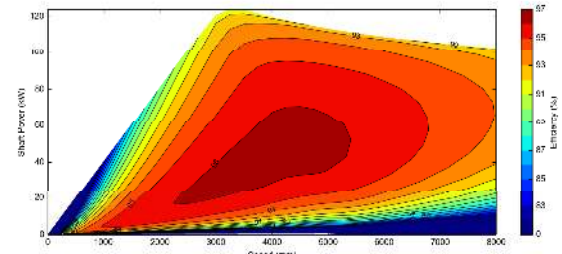
(b) Peak power

Figure 19 Peak performance for a synchronous IPM motor PHEV

(a) Continuous torque comparison

(b) Continuous power comparison

Figure 20 Continuous performance for a synchronous IPM motor PHEV

The latter system has good but limited capability of heat extraction on its own and is recommended to be used in conjunction with the oil spray cooling systems. When both

cooling elements are active, the maximum continuous torque increases from 185Nm to 315Nm, while the maximum continuous power sees an increase from 68kW to 98kW.

IV. MILD HYBRID ELECTRICAL VEHICLES SOLUTIONS

One possible design for the MHEV specification is a synchronous PM motor and is based on the equivalent Honda Accord motor [6]. Considering the specifications from Table VIII, we can investigate the peak and continuous performance of the synchronous PM, when two materials are used for the stator winding: (a) copper; (b) pressed aluminium coils. The pressed aluminium winding is a technology that would allow packing more material in a pre-formed coil and hence reducing the resistance of the coil, while increasing the thermal conductivity through a better contact between wires [7, 17]

The main design parameters of the synchronous permanent motor MHEV solution are listed in Table IX.

TABLE VIII – MHEV POWER TRAIN SPECIFICATIONS

Parameter	Unit	Value
Peak torque	Nm	125
Peak power	kW	25
DC bus voltage	V	144
Maximum speed	rpm	6000
Maximum current	Arms	180
Axial active length	mm	~40
Cooling system	N/A	Water jacket (EGW)

TABLE IX – MHEV SYNCHRONOUS PM MOTOR DETAILS

Parameter	Unit	Value
Stator OD	mm	315.5
Stator ID	mm	232
Airgap	mm	1.0
Slots	/	24
Poles	/	16
Electric steel	/	M270-35A
Magnet	/	N30UH

TABLE X – LOSS/WEIGHT COMPARISON IN MHEV SOLUTION AT: (A) 75NM AND 2000RPM; (B) 40NM AND 6000RPM

Winding material	Copper	Pressed Aluminum
DC Joule loss (W) (A)	372.5	543.4
DC Joule loss (W) (B)	982	1418
AC Joule loss (W) (A)	15.58	12.67
AC Joule loss (W) (B)	325	264
Weight (kg)	3.12	1.10
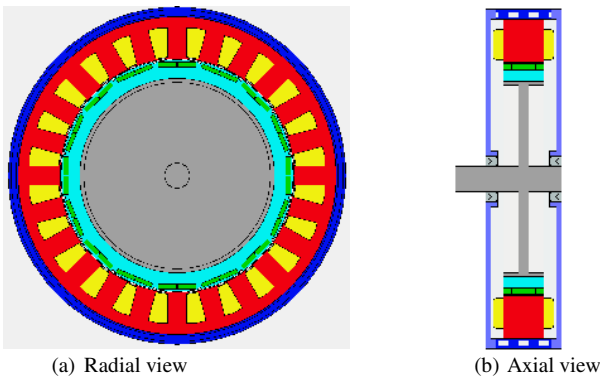
(a) Radial view (b) Axial view
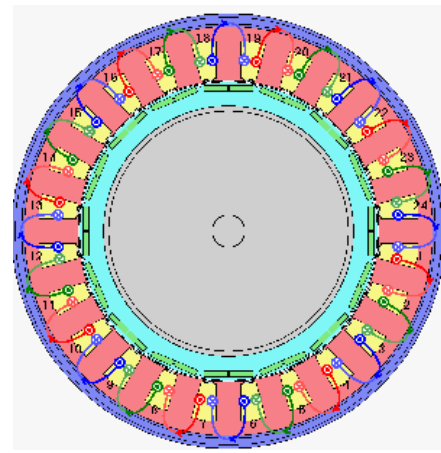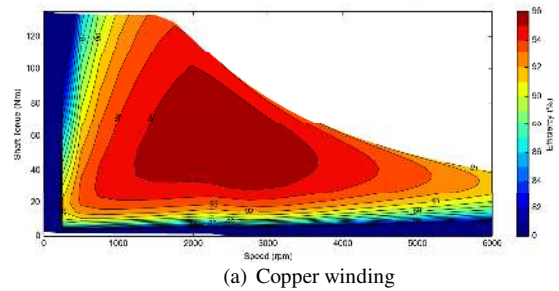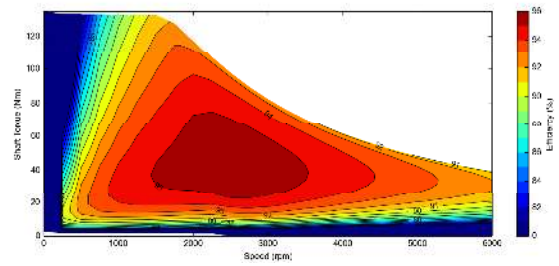
Figure 21 Synchronous PM for MHEV

Figure 22 Winding pattern (16 poles, double layer) for synchronous PM motor
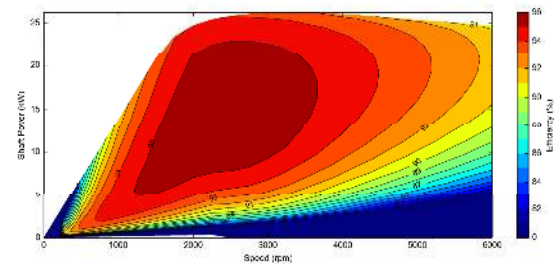

(a) Copper winding

(b) Aluminum winding

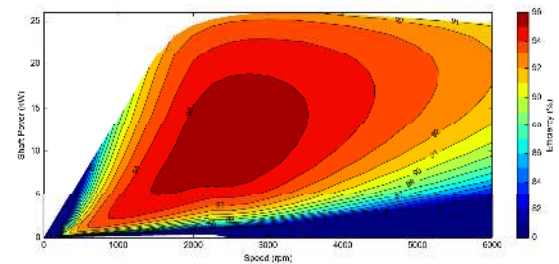Figure 23 Peak torque performance for a synchronous PM motor MHEV

(a) Copper winding

Figure 24 Peak power performance for a synchronous PM motor MHEV

Fig. 21 shows the radial and axial view of the the synchronous PM motor solution. The winding pattern (Fig. 20) consists of a concentrated set of tooth wound coils per pole and per phase, with 52 turns per coil. There are 8 parallel paths in the 3-phase winding system. Two winding types are considered: one with stranded round copper wire, size 1.5mm and slot fill factor 0.40; one with pressed aluminium wire, size 1.6mm and slot fill factor 0.46.

The cooling system comprises one elements: spiral stator water jacket that is using forced convection with water ethylene glycol mixture (50%-50%) as heat extraction fluid and an inlet temperature of 65 ^{0}C. It is assumed a fluid flow rate of 6 liters/min.

The results comparison in Figs. 23 and 24 shows that the peak performance at 100^{0}C overall temperature, is achieved in a similar mode regardless of the winding material.
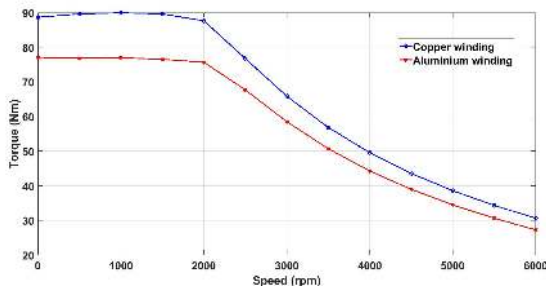

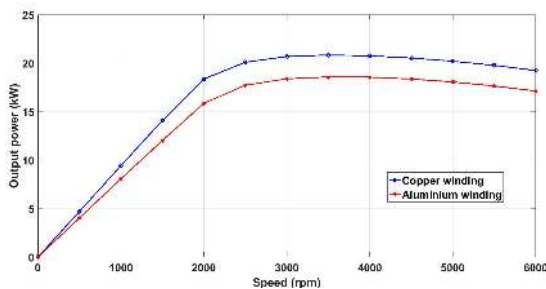Figure 25 Continuous torque performance for a synchronous PM motor MHEV

Figure 26 Continuous power performance for a synchronous PM motor MHEV

The difference in performance appears as for the previously analyzed cases (BEV and PHEV) at continuous operation (Figs. 25 and 26). The thermal limits and the efficiency of the cooling system in extracting the heat generated by losses will determine the maximum continuous torque and power values.

In this proposed MHEV design, as expected the copper winding will lead to higher continuous operation limit as compared to an aluminum winding case, i.e. 89Nm and 20kW vs 78Nm and 18kW. However, considering the cost reduction and weight saving in winding (Table X), 3.12kg stator copper vs 1.10kg stator aluminum, the decrease in performance may be acceptable.

V. Conclusions

A review of various solutions for power traction motors in electrical and hybrid vehicles is presented. Based on

equivalent designs to actual vehicles like Tesla S, Nissan Leaf, Chevrolet Volt and Honda Accord, this paper investigates the effect of various winding topologies in a battery electrical vehicle, cooling system in plug-in hybrid electric vehicle, and winding material in mild hybrid electric vehicle.

The magnet free electrical motors – induction and synchronous wound field – represent viable alternatives to rare-earth magnet motors in power traction applications. A novel solution to improve the performance of these machines is the usage of flat wire – hairpin – windings. Such solution was successfully implemented in brushless permanent magnet machines, but not with induction or synchronous wound field machines that are used in existing power traction systems. It is shown that when moving from a stranded wire winding design to one with flat wire – hairpin – winding, it is preferable to keep the same slot area and not the copper area. Only then, the reduction the DC copper losses will overcome the increase in AC losses, such that the motor overall performance will be improved.

Oil spray cooling systems are cheaper to implement and could improve significantly the performance of a traction motors if used as a secondary mode to extract the heat. As a standalone cooling system, the oil spray cooling shows very good potential in a how much heat can be dissipated from the system.

A cheap alternative in reducing the weight and cost for traction motors, can be the usage of pressed aluminum winding coils. Even if the performance at thermal steady-state is reduced in comparison with copper winding coils, the cost and weight reduction may lead to preferred solution for lower power, lower end traction applications, e.g. small transportation vehicles or electric bikes.

VI. References

[1] "The roadmap for transforming the EU into a competitive, low-carbon economy by 2050" (ec.europa.eu/clima/sites/clima/)
[2] K-C Kim, "Driving Characteristic Analysis of Traction Motors for Electric Vehicle by using FEM", Ansys Users Conference, Seoul, Korea, October 2014
[3] Y. Sato et al, "Development of High Response Motor and Inverter System for the Nissan LEAF Electric Vehicle", International World Congress and Exhibition, Detroit, April 2011
[4] BMW documentation (bmw.com/com/en/newvehicles/i/i3/2013)
[5] S. Jurkovic, K. Rahman, B. Bae, N. Patel and P. Savagian, "Next generation Chevy Volt electric machines; design, optimization and control for performance and rare-earth mitigation," *IEEE ECCE* Montreal, 2015, pp. 5219-5226.
[6] T. Burress et al, "Benchmarking of Competitive Technologies", Oak Ridge National Laboratory, May 2012.
[7] J.D. Widmer, R. Martin, and M. Kimiabeigi "Electric vehicle traction motors without rare earth magnets" *Sustainable Materials and Technologies*, No *3*, 2015, pp.7-13.
[8] E.A. Grunditz, T. Thiringer, "Performance Analysis of Current BEVs Based on a Comprehensive Review of Specifications", *IEEE Trans. On Transportation Electrification,* Vol. Vol. 2, No. 3, Sept. 2016, pp. 270-289
[9] J. Goss, R. Wrobel, P. Mellor, and D. Staton, "The Design of AC Permanent Magnet Motors for Electric Vehicles: A Design Methodology", in *IEEE IEMDC*, Chicago, May 2013
[10] J. Goss, P. H. Mellor, R. Wrobel, D. A. Staton, and M.Popescu, "The design of AC permanent magnet motors for electric vehicles: a

computationally efficient model of the operational envelope," in *6th IET International Conference on Power Electronics, Machines and Drives (PEMD 2012)*, 2012, pp. B21–B21.

[11] A. Mahmoudi, W. L. Soong, G. Pellegrino, and E. Armando, "Efficiency maps of electrical machines," in *2015 IEEE Energy Conversion Congress and Exposition (ECCE)*, 2015, pp. 2791–2799.

[12] J. Goss, M. Popescu, D. Staton, P. H. Mellor, R. Wrobel, and J. Yon, "A Comparison between Maximum Torque/Ampere and Maximum Efficiency Control Strategies in IPM Synchronous Machines," in *IEEE Energy Conversion Congress and Exposition (ECCE)*, 2014.

[13] S.H. Swales et al, "Oil cooled motor/generator for an automotive powertrain", US patent application #US 8169110 B2

[14] L. Fedoseyev and E.M. Pearce Jr."Rotor assembly with heat pipe cooling system", US patent application # 2014/0368064 A1

[15] Cai, W. and Fulton, D. and Congdon, C.L. "Multi-set rectangular copper hairpin windings for electric machines", US patent # 6,894,417, 2005

[16] Guercioni, S. "Methods for twisting rotor and stator ends", US patent # 8,215,000, 2012

[17] M. Popescu, D. A. Staton, A. Boglietti, A. Cavagnino, D. Hawkins and J. Goss, "Modern Heat Extraction Systems for Power Traction Machines—A Review," in *IEEE Transactions on Industry Applications*, vol. 52, no. 3, pp. 2167-2175, May-June 2016.doi: 10.1109/TIA.2016.2518132

[18] J. Goss, M. Popescu, D. Staton, D. Hawkins, A. Boglietti, "Electrical vehicles - practical solutions for power traction drive systems," 2017 *IEEE Workshop on Elec. Machines Design, Control and Diag. (WEMDCD)*, Nottingham, U.K., pp. 80 – 88